Electronic Supplementary Material (ESI) for Journal of Materials Chemistry B.

Supporting Information

Biflavones inhibit the fibrillation and cytotoxicity of human islet amyloid polypeptide

Jufei Xu, Yanan Wang, Ting Zheng, Yan Huo, Weihong Du*

Department of Chemistry, Renmin University of China, Beijing, 100872, China

Table S1. Height analysis of peptide aggregates along with lines marked in Fig. 3.

Biflavones	Ratio	hIAPP	
	B/p*	Position	Height[a] / nm
0	0:1	a	11.8
1	1:1	b	30.8
	5:1	c	20.9
	10:1	d	7.7
2	1:1	e	13.4
	5:1	f	9.7
	10:1	g	8.5

[a] Values were determined by the AFM. * B/p means the molar ratio of biflavones to peptides.

Table S2. Analysis of the favored and additional allowed regions in Ramachandran plot.

Compds	*Regions	No. of residues	Tag / %
hIAPP22-28	Most favored [A, B, L]	31	96.9
	Additional allowed [a, b, l, p]	1	3.1
	Generously allowed [~a, ~b, ~l, ~p]	0	0.0
	Disallowed [XX]	0	0.0
1+hIAPP22-28	Most favoured [A, B, L]	28	87.5
	Additional allowed [a, b, l, p]	4	12.5
	Generously allowed [~a, ~b, ~l, ~p]	0	0.0
	Disallowed [XX]	0	0.0
2+hIAPP22-28	Most favoured [A, B, L]	29	90.6
	Additional allowed [a, b, l, p]	3	9.4
	Generously allowed [~a, ~b, ~l, ~p]	0	0.0
	Disallowed [XX]	0	0.0

* The residues glycine and proline were excluded.

Table S3. Contact probability of hIAPP22−28 octamer with biflavones in MD simulation.

Biflavones	Chain-residues	Contact probability %	Biflavones	Chain-residues	Contact probability %
1+hIAPP22−28	a*-Ile26	47.87	**2**+hIAPP22−28	c-Leu27	31.57
	g-Phe23	34.84		g-Phe23	26.33
	b-Phe23	34.39		g-Leu27	25.19
	e-Ile26	33.65		d-Asn22	24.62
	d-Phe23	31.58		c-Phe23	24.09
	a-Leu27	23.75		a-Leu27	23.90
	c-Asn22	20.43		h-Phe23	22.95
	g-Ile26	18.29		h-Leu27	20.05

* The letters from a to h refer to each of the octamer chains.

Table S4. Contact distance of Phe23 residues in hIAPP22−28 octamers with biflavones in MD simulation.

Biflavones	Contact residues:**1**	Avg distance(Å)	Biflavones	Contact residues:**2**	Avg distance(Å)
1+hIAPP22−28	g*-Phe23-CA:**1**-O4	3.82	**2**+hIAPP22−28	g-Phe23-CA:**2**-H14	3.60
	g-Phe23-CA:**1**-H12	3.87		g-Phe23-CA:**2**-H20	3.98
	g-Phe23-CA:**1**-O3	4.05		g-Phe23-CA:**2**-C21	4.28
	g-Phe23-CA:**1**-H10	4.08		g-Phe23-CA:**2**-O7	4.57
	g-Phe23-CA:**1**-H4	4.65		g-Phe23-CA:**2**-C20	4.77
	g-Phe23-CA:**1**-C8	4.71		g-Phe23-CA:**2**-C17	4.89
	g-Phe23-CA:**1**-C15	4.97		g-Phe23-CA:**2**-O10	4.95

* The letters from a to h refer to each of the octamer chains.

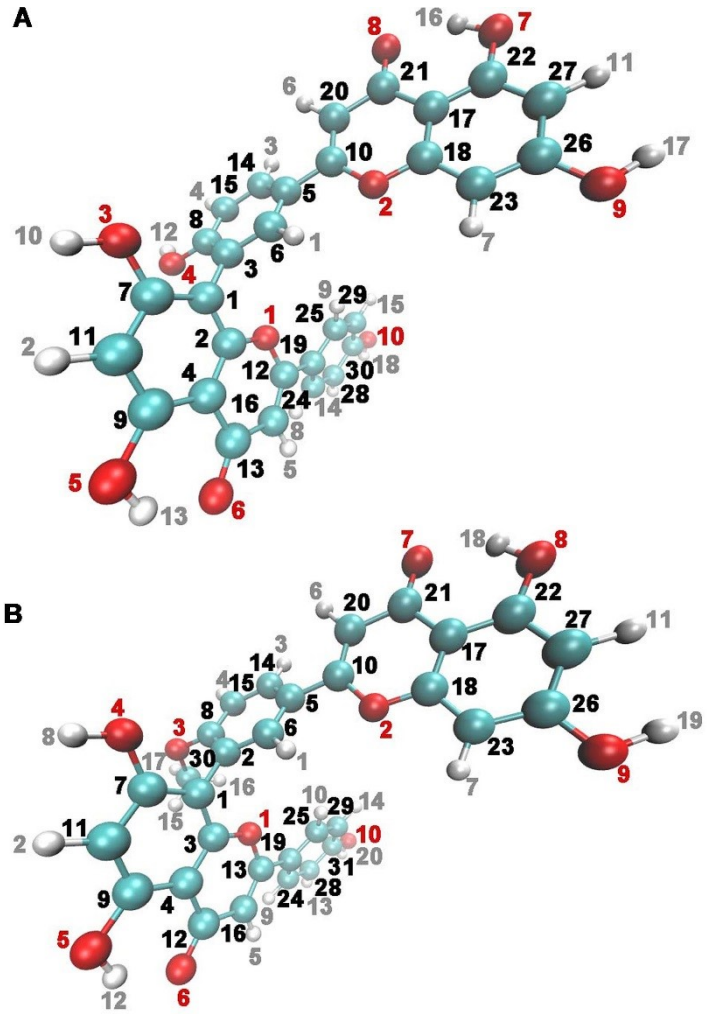

Scheme S1. The atoms nomenclature of **1** (A), and **2** (B) marked in MD simulation.

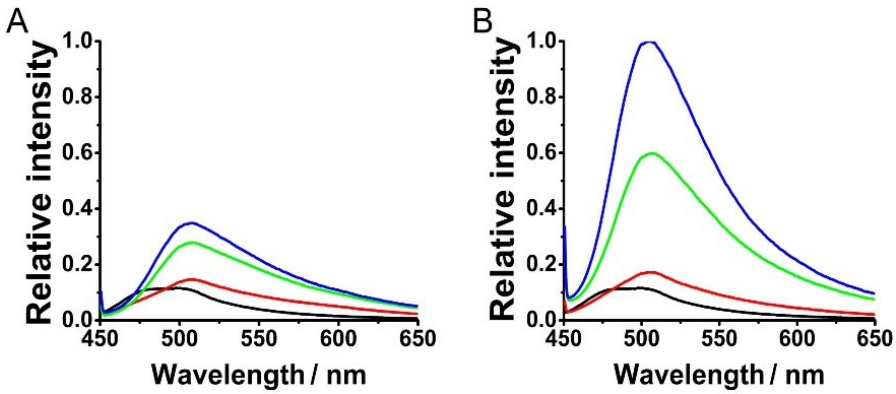

Fig. S1. The fluorescence spectra of 10 μM ThT in the absence (black) or presence of 5 (red), 25 (green), and 50 μM (blue) of **1** (A) and **2** (B) in 10 mM PB, pH 7.4.

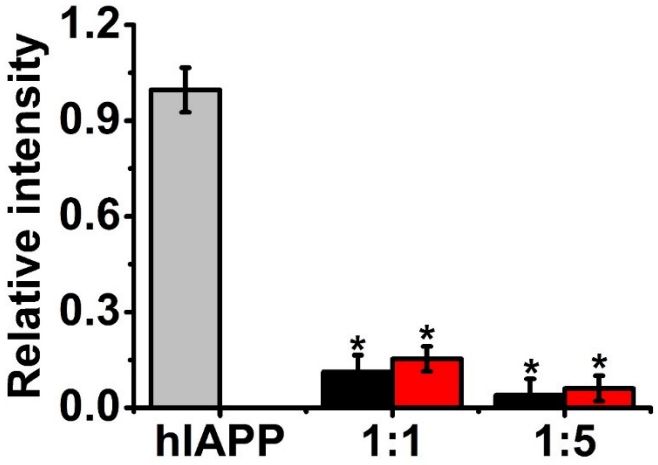

Fig. S2. ThT fluorescence assay of 5 μM hIAPP (A, B) disaggregation in the absence (grey) or presence of equivalent and fivefold of **1** (black), and **2** (red) in 10 mM PB, pH 7.4. The concentration of ThT was 10 μM in solution. The peak intensity was recorded at 484 nm.

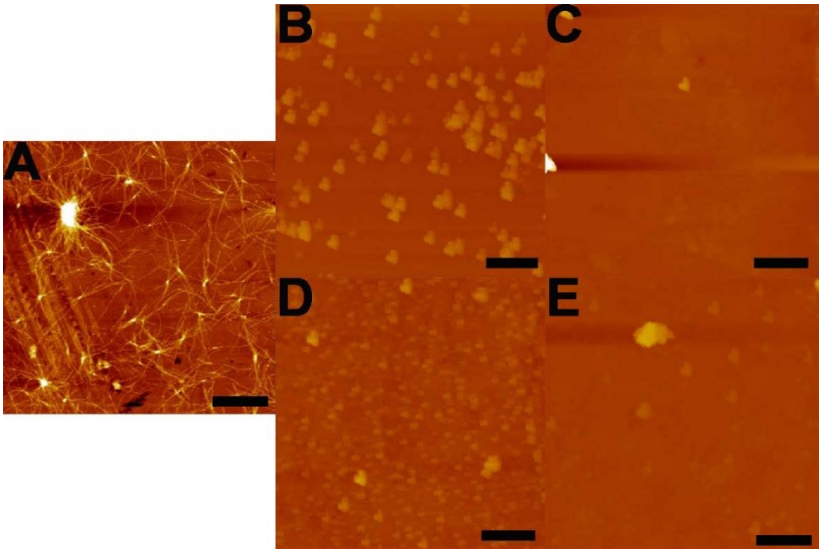

Fig. S3. AFM images of 5 μM hIAPP disaggregation in the absence (A) or presence of equivalent (B, D), and fivefold amounts (C, E) of **1** (B, C), and **2** (D, E). The scale bar is 2 μm.

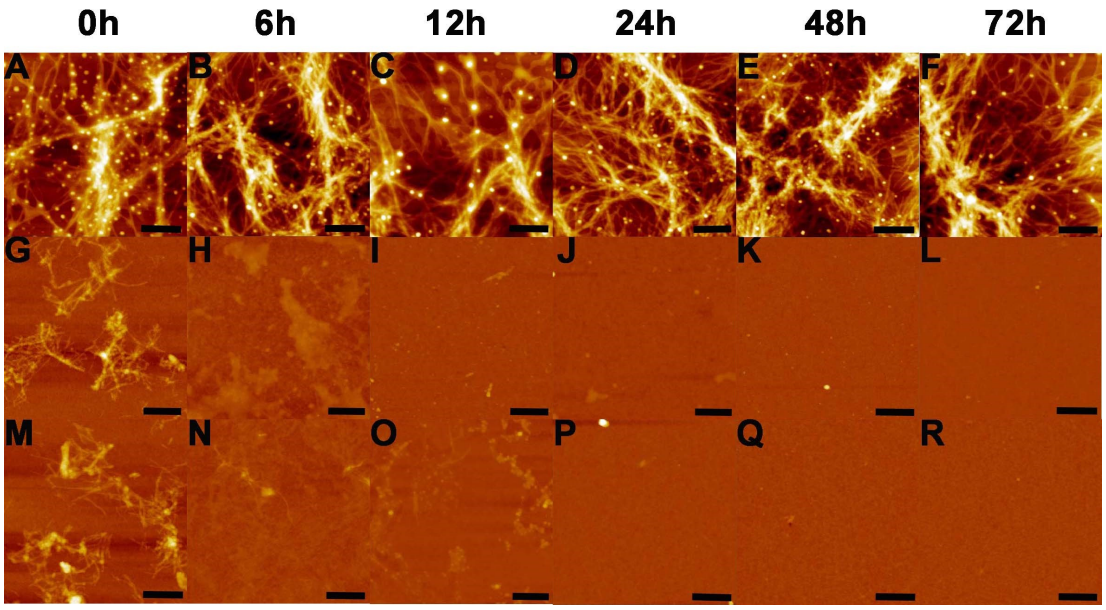

Fig. S4. AFM images of time-dependent disaggregation of 5 μM hIAPP in the absence (A-F) or presence of fivefold excess of **1** (G-L), and **2** (M-R) (25 μM) at 0, 6, 12, 24, 48, and 72 h.

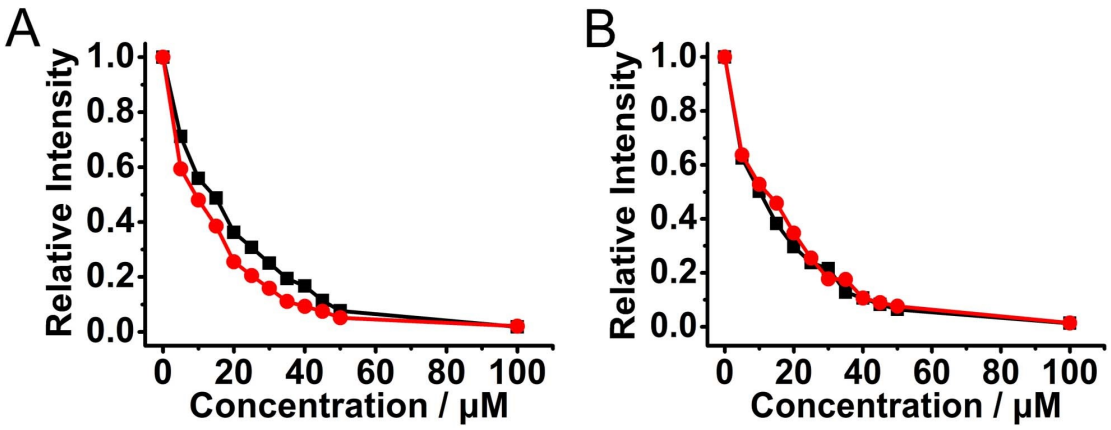

Fig. S5. Intrinsic fluorescence quenching of 10 μM hIAPP in the presence of **1** (black) and **2** (red) (0–100 μM) in 10 (A) and 100 mM PB (B) determined at pH 7.4 and 25°C. The excitation and emission wavelengths were 275 nm and 305 nm, respectively.

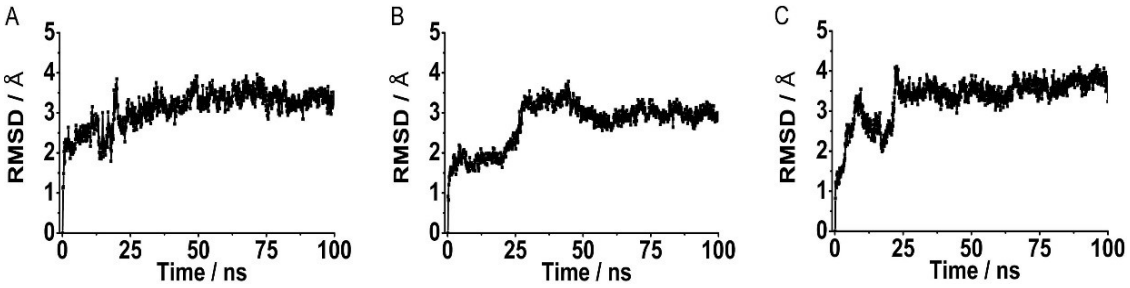

Fig. S6. RMSD of hIAPP22−28 octamer in the absence (A) or presence of fivefold excess of **1** (B) and **2** (C).

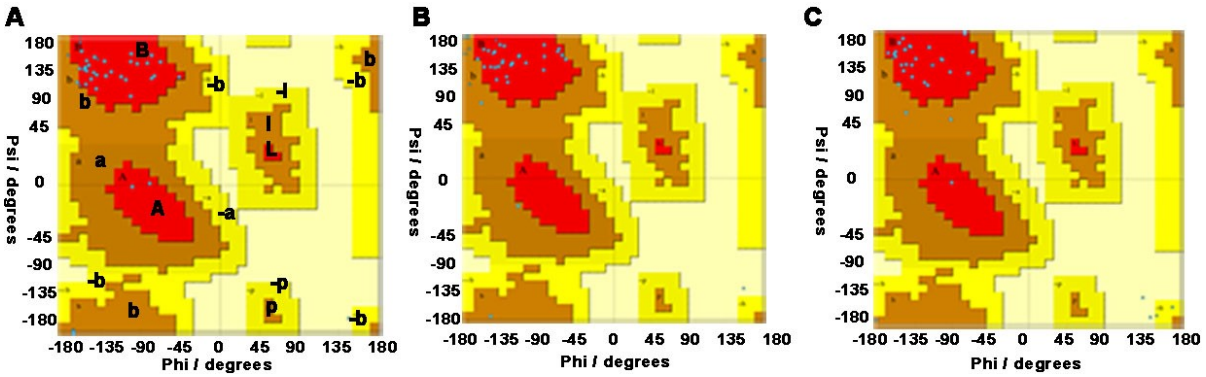

Fig. S7. Ramachandran plot maps of hIAPP22−28 octamer in the absence (A) or presence of fivefold excess of **1** (B) and **2** (C). The blue tag represents each amino acid. A-core alpha, B-core beta, L- core left-handed alpha; a-allowed alpha, b-allowed beta, l-allowed left-handed alpha, p-allowed epsilon; ~a-generous alpha, ~b-generous beta, ~l-generous left-handed alpha, ~p-generous epsilon. All the regions correspond to each other.

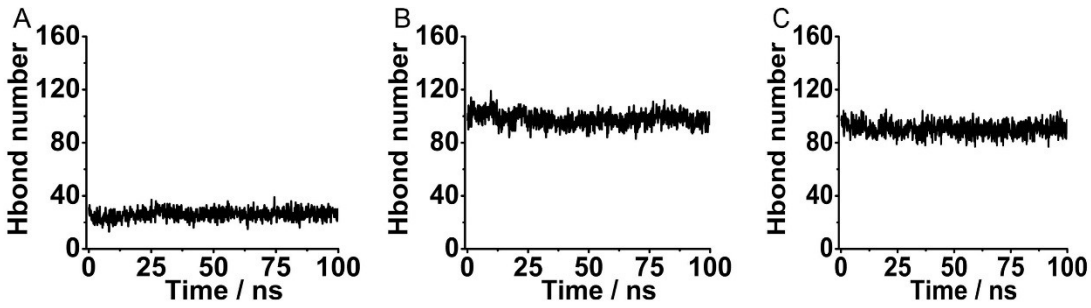

Fig. S8. Hydrogen bond number of hIAPP22−28 octamer in the absence (A) or presence of fivefold excess of **1** (B), and **2** (C) in 100 ns MD run.

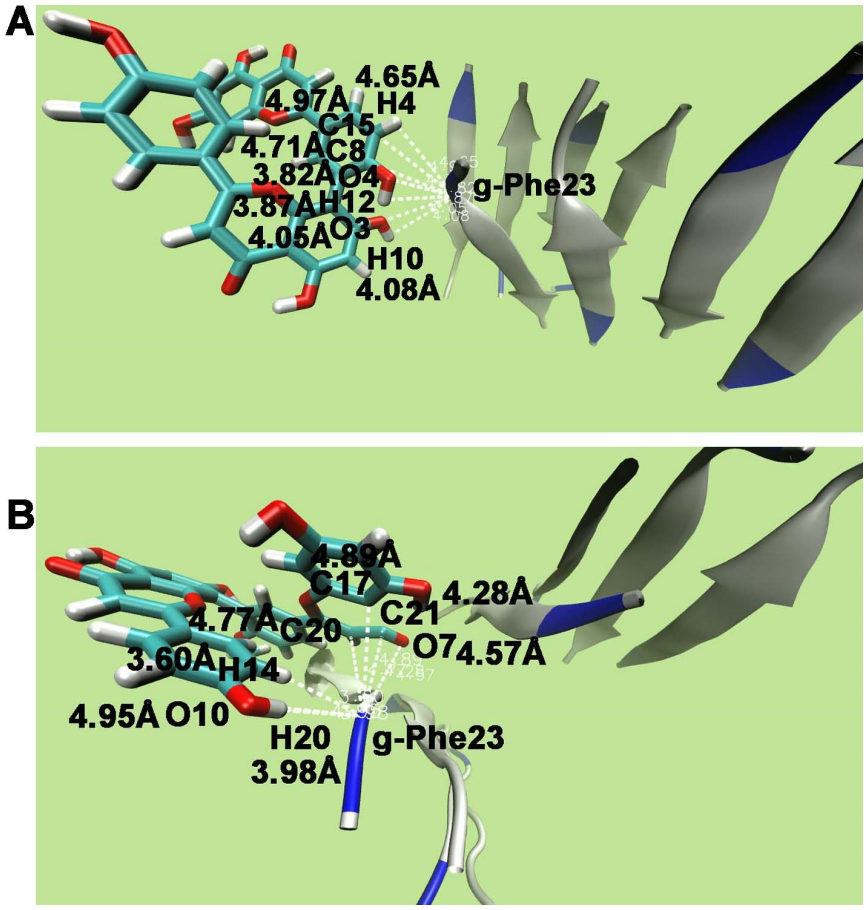

Fig. S9. Contact distribution of Phe23 residues in hIAPP22−28 octamer (gray) in the presence of fivefold excess of **1** (A) and **2** (B). The Phe23 (blue) residues were labelled in all the peptide chains. The white dotted lines represent the contact distance between the Phe23 residue and the atoms of biflavones.

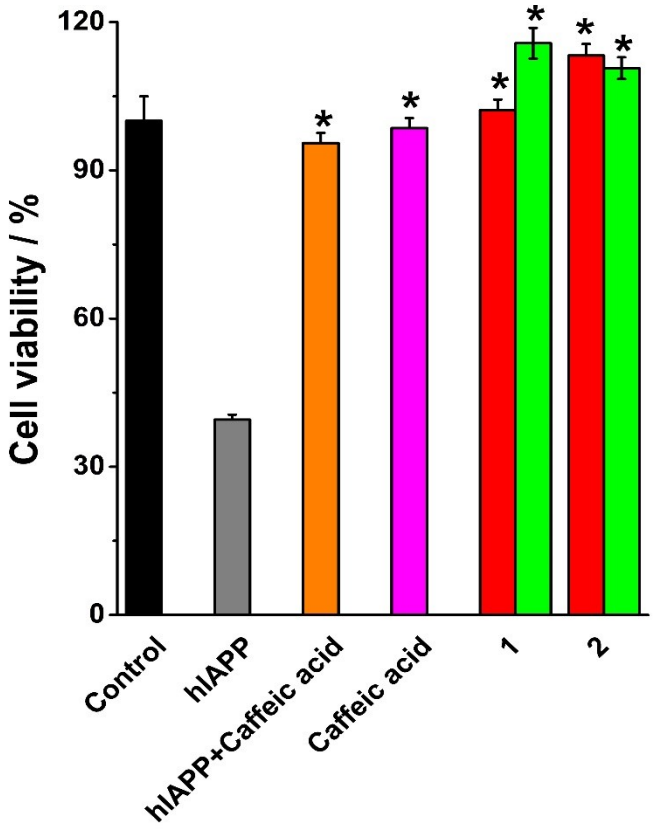

Fig. S10. The viability of INS−1 cells with 15 μM hIAPP in the absence (grey) and presence of **1** and **2** alone at 1.5 (red), and 15.0 μM (green), respectively. The negative control was obtained by incubating 15 μM caffeic acid with hIAPP (orange). Data analysis presents means ± S. E. M. with n = 3. *$p < 0.05$ by one−way ANOVA in IBM SPSS Statistics 17.0. The marked is of significant difference compared with hIAPP alone (grey).

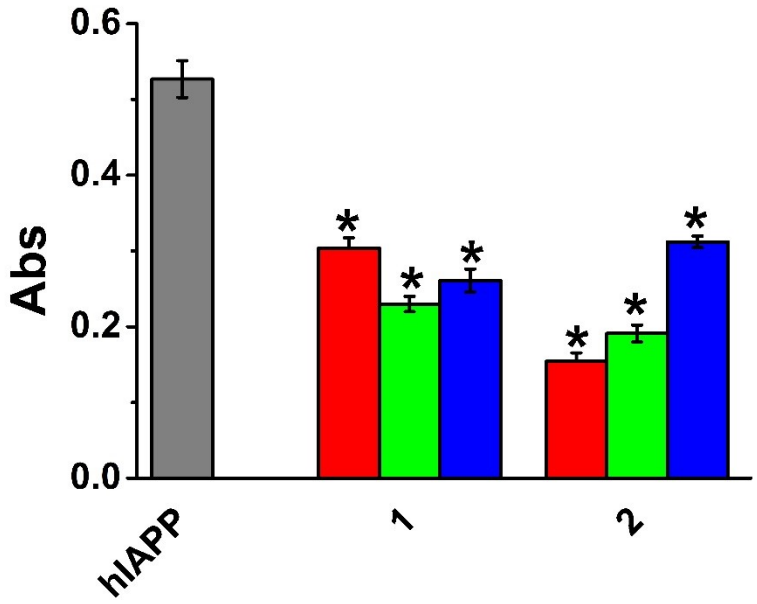

Fig. S11. ELISA assay of A−11 antibodies with 100 μM hIAPP in the absence (gray) and presence of 50 (red), 100 (green), and 200 μM (blue) of **1** and **2** alone, respectively. Data are shown as means ± SD, n=3 in normal distribution, *$p < 0.05$ by one−way ANOVA in IBM SPSS Statistics 17.0. The marked is of significant difference compared with hIAPP (grey).